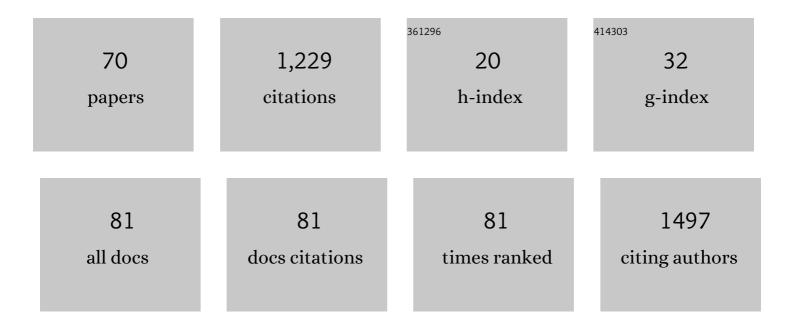
## Antoine Simon

List of Publications by Year in descending order

Source: https://exaly.com/author-pdf/489802/publications.pdf Version: 2024-02-01



#	Article	IF	CITATIONS
1	Preterm Newborn Presence Detection in Incubator and Open Bed Using Deep Transfer Learning. IEEE Journal of Biomedical and Health Informatics, 2021, 25, 1419-1428.	3.9	5
2	Fusion of 3D real-time echocardiography and cine MRI using a saliency analysis. International Journal of Computer Assisted Radiology and Surgery, 2020, 15, 277-285.	1.7	6
3	Planning With Patient-Specific Rectal Sub-Region Constraints Decreases Probability of Toxicity in Prostate Cancer Radiotherapy. Frontiers in Oncology, 2020, 10, 1597.	1.3	4
4	Comparison of CBCTâ€based dose calculation methods in head and neck cancer radiotherapy: from Hounsfield unit to density calibration curve to deep learning. Medical Physics, 2020, 47, 4683-4693.	1.6	43
5	Cardiac Cine-MRI/CT Registration for Interventions Planning. , 2019, , .		1
6	Video and audio processing in paediatrics: a review. Physiological Measurement, 2019, 40, 02TR02.	1.2	31
7	Deformable image registration for radiation therapy: principle, methods, applications and evaluation. Acta Oncológica, 2019, 58, 1225-1237.	0.8	74
8	Deformable image registration for dose mapping between external beam radiotherapy and brachytherapy images of cervical cancer. Physics in Medicine and Biology, 2019, 64, 115023.	1.6	18
9	Statistical Shape Model to Generate a Planning Library for Cervical Adaptive Radiotherapy. IEEE Transactions on Medical Imaging, 2019, 38, 406-416.	5.4	31
10	CBCTâ€guided evolutive library for cervical adaptive IMRT. Medical Physics, 2018, 45, 1379-1390.	1.6	23
11	PO-1078: CBCT guided adaptive radiotherapy for cervix cancer: Uncertainty of the choice of the plan of the day. Radiotherapy and Oncology, 2018, 127, S606-S607.	0.3	2
12	Multimodal Image Fusion for Cardiac Resynchronization Therapy Planning. , 2018, , 67-82.		0
13	Treatment plan library based on population shape analysis for cervical adaptive radiotherapy. , 2018, , .		0
14	MRI to CT Prostate Registration for Improved Targeting in Cancer External Beam Radiotherapy. IEEE Journal of Biomedical and Health Informatics, 2017, 21, 1015-1026.	3.9	22
15	ls Dose Deformation–Invariance Hypothesis Verified in Prostate IGRT?. International Journal of Radiation Oncology Biology Physics, 2017, 97, 830-838.	0.4	3
16	Population model of bladder motion and deformation based on dominant eigenmodes and mixed-effects models in prostate cancer radiotherapy. Medical Image Analysis, 2017, 38, 133-149.	7.0	17
17	PO-0841: Feasibility of dose decrease in a rectal subregion predictive of bleeding in prostate radiotherapy. Radiotherapy and Oncology, 2017, 123, S454-S455.	0.3	1
18	PO-1017: Dose guided adaptive radiotherapy based on cumulated dose in OAR for prostate cancer. Radiotherapy and Oncology, 2017, 123, S561-S562.	0.3	0

#	Article	IF	CITATIONS
19	OC-0352: CBCT-guided evolutive library for cervix adaptive IMRT. Radiotherapy and Oncology, 2017, 123, S186-S187.	0.3	2
20	Pseudo-CT generation by conditional inference random forest for MRI-based radiotherapy treatment planning. , 2017, , .		5
21	The benefit of using bladder sub-volume equivalent uniform dose constraints in prostate intensity-modulated radiotherapy planning. OncoTargets and Therapy, 2016, Volume 9, 7537-7544.	1.0	14
22	Optimal adaptive IMRT strategy to spare the parotid glands in oropharyngeal cancer. Radiotherapy and Oncology, 2016, 120, 41-47.	0.3	46
23	Interindividual registration and dose mapping for voxelwise population analysis of rectal toxicity in prostate cancer radiotherapy. Medical Physics, 2016, 43, 2721-2730.	1.6	25
24	Identification of a rectal subregion highly predictive of rectal bleeding in prostate cancer IMRT. Radiotherapy and Oncology, 2016, 119, 388-397.	0.3	48
25	PO-0911: Optimal adaptive radiotherapy strategy in head and neck to spare the parotid glands. Radiotherapy and Oncology, 2016, 119, S439-S440.	0.3	0
26	Slice correspondence estimation using SURF descriptors and context-based search for prostate whole-mount histology MRI registration. , 2016, 2016, 1163-1166.		3
27	Overview of the predictive value of quantitative 18 FDG PET in head and neck cancer treated with chemoradiotherapy. Critical Reviews in Oncology/Hematology, 2016, 108, 40-51.	2.0	52
28	Detection of bladder metabolic artifacts in 18F-FDG PET imaging. Computers in Biology and Medicine, 2016, 71, 77-85.	3.9	8
29	Quantification of dose uncertainties in cumulated dose estimation compared to planned dose in prostate IMRT. Radiotherapy and Oncology, 2016, 119, 129-136.	0.3	44
30	Synchronization and Registration of Cine Magnetic Resonance and Dynamic Computed Tomography Images of the Heart. IEEE Journal of Biomedical and Health Informatics, 2016, 20, 1369-1376.	3.9	8
31	Registration of dynamic multiview 2D ultrasound and late gadolinium enhanced images of the heart: Application to hypertrophic cardiomyopathy characterization. Medical Image Analysis, 2016, 28, 13-21.	7.0	9
32	Improving the UAS-S4 Éhecal airfoil high angles-of-attack performance characteristics using a morphing wing approach. Proceedings of the Institution of Mechanical Engineers, Part G: Journal of Aerospace Engineering, 2016, 230, 118-131.	0.7	17
33	Roles of Deformable Image Registration in adaptive RT: From Contour propagation to dose monitoring. , 2015, 2015, 5215-8.		10
34	Evaluation of Deformable Image Registration Methods for Dose Monitoring in Head and Neck Radiotherapy. BioMed Research International, 2015, 2015, 1-16.	0.9	53
35	Prostate whole-mount histology reconstruction and registration to MRI for correlating in-vivo observations with biological findings. , 2015, 2015, 2399-402.		7
36	Multi-modal data fusion for Cardiac Resynchronization Therapy planning and assistance. , 2015, 2015,		1

<sup>36</sup> 2391-4.

#	Article	IF	CITATIONS
37	Impact of head and neck cancer adaptive radiotherapy to spare the parotid glands and decrease the risk of xerostomia. Radiation Oncology, 2015, 10, 6.	1.2	117
38	Dosimetric Benefit of Adaptive Radiation Therapy With Reduced Planning Target Volume Margins in Cervix Carcinoma. International Journal of Radiation Oncology Biology Physics, 2015, 93, E271-E272.	0.4	2
39	The role of imaging in adaptive radiotherapy for head and neck cancer. Irbm, 2014, 35, 33-40.	3.7	6
40	Multimodal Registration and Data Fusion for Cardiac Resynchronization Therapy Optimization. IEEE Transactions on Medical Imaging, 2014, 33, 1363-1372.	5.4	26
41	Segmentation of pelvic structures for planning CT using a geometrical shape model tuned by a multi-scale edge detector. Physics in Medicine and Biology, 2014, 59, 1471-1484.	1.6	38
42	Surface-Constrained Nonrigid Registration for Dose Monitoring in Prostate Cancer Radiotherapy. IEEE Transactions on Medical Imaging, 2014, 33, 1464-1474.	5.4	23
43	A new pencil beam model for photon dose calculations in heterogeneous media. Physica Medica, 2014, 30, 765-773.	0.4	2
44	Random Forests to Predict Rectal Toxicity Following Prostate Cancer Radiation Therapy. International Journal of Radiation Oncology Biology Physics, 2014, 89, 1024-1031.	0.4	45
45	Gradient Collinearity Method for Prostate MRI to CT Registration. International Journal of Radiation Oncology Biology Physics, 2014, 90, S438.	0.4	0
46	Multi-Atlas-Based Segmentation of Pelvic Structures from CT Scans for Planning in Prostate Cancer Radiotherapy. , 2014, , 623-656.		20
47	Investigating the contribution of pre- and per-treatment 18F-FDG PET-CT segmentation methodologies for post-treatment tumor recurrence prediction in cervical cancer. Irbm, 2013, 34, 274-277.	3.7	3
48	Voxel-based population analysis for correlating local dose and rectal toxicity in prostate cancer radiotherapy. Physics in Medicine and Biology, 2013, 58, 2581-2595.	1.6	66
49	A new pencil beam model for photon dose calculations. , 2013, , .		0
50	Nomograms to predict late urinary toxicity after prostate cancer radiotherapy. World Journal of Urology, 2013, 32, 743-51.	1.2	33
51	Evaluation of non-rigid constrained CT/CBCT registration algorithms for delineation propagation in the context of prostate cancer radiotherapy. Proceedings of SPIE, 2013, , .	0.8	5
52	A new deconvolution approach to robust fluence for intensity modulation under geometrical uncertainty. Physics in Medicine and Biology, 2013, 58, 6095-6110.	1.6	1
53	Propagation of the MRI prostate delineation to the planning CT: A new matching contour framework. , 2013, , .		2
54	Evaluation of a motion artifacts removal approach on breath-hold cine-magnetic resonance images of hypertrophic cardiomyopathy subjects. , 2013, , .		1

#	Article	IF	CITATIONS
55	Impact of MLC leaf width on volumetricâ€modulated arc therapy planning for head and neck cancers. Journal of Applied Clinical Medical Physics, 2013, 14, 40-52.	0.8	18
56	A Tensor-Based Population Value Decomposition to Explain Rectal Toxicity after Prostate Cancer Radiotherapy. Lecture Notes in Computer Science, 2013, 16, 387-394.	1.0	4
57	Spatio-temporal Registration of 2D US and 3D MR Images for the Characterization of Hypertrophic Cardiomyopathy. Lecture Notes in Computer Science, 2013, , 292-299.	1.0	2
58	Inter-individual organ-driven CT registration for dose mapping in prostate cancer radiotherapy. , 2012, , .		3
59	Evaluation of inter-individual pelvic CT-scans registration. Irbm, 2011, 32, 288-292.	3.7	6
60	Evaluation of multi-atlas-based segmentation of CT scans in prostate cancer radiotherapy. , 2011, , .		23
61	Spatial Nonparametric Mixed-Effects Model with Spatial-Varying Coefficients for Analysis of Populations. Lecture Notes in Computer Science, 2011, , 142-150.	1.0	4
62	Spatial Characterization and Classification of Rectal Bleeding in Prostate Cancer Radiotherapy with a Voxel-Based Principal Components Analysis Model for 3D Dose Distribution. Lecture Notes in Computer Science, 2011, , 60-69.	1.0	10
63	Dose Monitoring in Prostate Cancer Radiotherapy Using CBCT to CT Constrained Elastic Image Registration. Lecture Notes in Computer Science, 2011, , 70-79.	1.0	4
64	Benefit of IMRT in High Dose Prostate Cancer Radiotherapy. International Journal of Radiation Oncology Biology Physics, 2010, 78, S352-S353.	0.4	3
65	Atlas Based Segmentation and Mapping of Organs at Risk from Planning CT for the Development of Voxel-Wise Predictive Models of Toxicity in Prostate Radiotherapy. Lecture Notes in Computer Science, 2010, , 42-51.	1.0	13
66	Data fusion of Left Ventricle Electro-Anatomical Mapping and Multislice Computerized Tomography. , 2009, , .		4
67	Three distinct sarcomeric patterns of skeletal muscle revealed by SHG and TPEF Microscopy. Optics Express, 2009, 17, 19763.	1.7	32
68	Cardiac function estimation for resynchronization therapy: Comparison between multislice-ct and speckle tracking imaging. , 2008, , .		1
69	Assessment of Left Ventricular Function in Cardiac MSCT Imaging by a 4D Hierarchical Surface-Volume Matching Process. International Journal of Biomedical Imaging, 2006, 2006, 1-10.	3.0	10
70	A Surface-Volume Matching Process Using a Markov Random Field Model for Cardiac Motion Extraction in MSCT Imaging. Lecture Notes in Computer Science, 2005, , 457-466.	1.0	4